The furnace temperature (middle) was set at 800 °C during growth, and the target was placed at the upstream end rather than middle of the furnace. A pulsed (8-ns, 10-Hz) Nd-YAG laser (wavelength 1,064 nm) was used to vaporize the target. Typically, growth was performed for 10 min with NWs collected at the downstream, cool end of the furnace.

Electrical characterization

Transport measurement on individual NWs were carried out using published procedures[11]. NWs were first dispersed in ethanol, and then deposited onto oxidized silicon substrates (600 nm oxide, 1–10 Ω cm resistivity), with the conductive silicon used as a back gate. Electrical contact to the NWs was defined using electron beam lithography (JEOL 6400). Ni/In/Au contact electrodes were thermally evaporated. Electrical transport measurements were made using a home-built system with <1 pA noise under computer control.

Junctions (n–n and p–p) were obtained by random deposition. We first deposited NWs onto oxidized silicon substrates using relatively high concentrations, determined the positions of crossed NWs, and then defined electrodes on all four arms of the cross by electron beam lithography. Ni/In/Au electrodes were used to make contact to the NWs.

p–n junctions were obtained by layer-by-layer deposition. First, a dilute solution of one type (for example, n-type) of NW was deposited on the substrate, and the positions of individual NWs were recorded. In a second step, a dilute solution of the other type (for example, p-type) of NW was deposited, and the positions of crossed n- and p-type NWs were recorded. Metal electrodes were then defined and transport behaviour was measured.

Optoelectrical characterization

EL was studied with a home-built micro-luminescence instrument[20]. PL or scattered light (514 nm, Ar-ion laser) was used to locate the position of the junction. When the junction was located, the excitation laser was shut off, and then the junction was forward biased. EL images were taken with a liquid-nitrogen-cooled CCD camera, and EL spectra were obtained by dispersing EL with a 150 lines mm^{-1} grating in a 300-mm spectrometer.

Received 11 July; accepted 25 October 2000.

1. Hu, J., Odom, T. W. & Lieber, C. M. Chemistry and physics in one dimension: synthesis and properties of nanowires and nanotubes. *Acc. Chem. Res.* **32,** 435–445 (1999).
2. Dekker, C. Carbon nanotubes as molecular quantum wires. *Phys. Today* **52**(5), 22–28 (1999).
3. Tans, S. J., Verschueren, R. M. & Dekker, C. Room temperature transistor based on a single carbon nanotube. *Nature* **393,** 49–52 (1998).
4. Martel, R., Schmidt, T., Shea, H. R., Hertel, T. & Avouris, P. Single- and multi-wall carbon nanotube field effect transistors. *Appl. Phys. Lett.* **73,** 2447–2449 (1998).
5. Tans, S. J. *et al.* Individual single-wall carbon nanotubes as quantum wires. *Nature* **386,** 474–477 (1997).
6. Bockrath, M. *et al.* Single electron transport in ropes of carbon nanotubes. *Science* **275,** 1922–1925 (1997).
7. Odom, T. W., Huang, J.-L., Kim, P. & Lieber, C. M. Atomic structure and electronic properties of single-walled carbon nanotubes. *Nature* **391,** 62–64 (1998).
8. Wildoer, J. W. G., Venema, L. C., Rinzler, A. G., Smalley, R. E. & Dekker, C. Electronic structure of atomically resolved carbon nanotubes. *Nature* **391,** 59–62 (1998).
9. Morales, A. M. & Lieber, C. M. A laser ablation method for the synthesis of crystalline semiconductor nanowires. *Science* **279,** 208–211 (1998).
10. Duan, X. & Lieber, C. M. General synthesis of compound semiconductor nanowires. *Adv. Mater.* **12,** 298–302 (2000).
11. Cui, Y., Duan, X., Hu, J. & Lieber, C. M. Doping and electrical transport in silicon nanowires. *J. Phys. Chem. B* **104,** 5213–5216 (2000).
12. Sze, S. M. *Physics of Semiconductor Devices* (Wiley, New York, 1981).
13. Alivisatos, A. P. Semiconductor clusters, nanocrystal, and quantum dots. *Science* **271,** 933–937 (1996).
14. Bolm, G. M. & Woodall, J. M. Efficient electroluminescence from InP diodes grown by liquid-phase epitaxy. *Appl. Phys. Lett.* **17,** 373–376 (1970).
15. Bessolov, V. N. & Lebedev, M. V. Chalcogenide passivation of III-V semiconductor surfaces. *Semiconductors* **32,** 1141–1156 (1998).
16. Micic, O. I., Sprague, J., Lu, Z. & Nozik, A. J. Highly efficient band edge emission from InP quantum dots. *Appl. Phys. Lett.* **68,** 3150–3152 (1996).
17. Smith, P. A. Electric-field assisted assembly and alignment of metallic nanowires. *Appl. Phys. Lett.* **77,** 1399–1401 (2000).
18. Xia, Y. N., Rogers, J. A., Paul K. E. & Whitesides, G. M. Unconventional methods for fabricating and patterning nanostructures. *Chem. Rev.* **99,** 1823–1848 (1999).
19. Duan, X. & Lieber, C. M. Laser assisted catalytic growth of single crystal GaN nanowires. *J. Am. Chem. Soc.* **122,** 188–189 (2000).
20. Duan, X., Wang, J. & Lieber, C. M. Synthesis and optical properties of GaAs nanowires. *Appl. Phys. Lett.* **76,** 1116–1168 (2000).

Supplementary information is available on *Nature*'s World-Wide Web site (http://www.nature.com) or as paper copy from the London editorial office of *Nature*.

Acknowledgements

We thank H. Park, M.S. Gudiksen, J.-L. Huang, K. Kim, T. Oosterkamp & S.-I. Yang for discussions. This work was supported by the US Office of Naval Research, Defense Advanced Projects Research Agency, and the National Science Foundation.

Correspondence and requests for materials should be addressed to C.M.L. (e-mail: cml@cmliris.harvard.edu).

Computational design of direct-bandgap semiconductors that lattice-match silicon

Peihong Zhang*, Vincent H. Crespi*, Eric Chang†, Steven G. Louie† & Marvin L. Cohen†

** Department of Physics, The Pennsylvania State University, 104 Davey Lab, University Park, Pennsylvania 16802-6300, USA*
† Department of Physics, University of California at Berkeley, Berkeley, California 94720 and Materials Sciences Division, Lawrence Berkeley Laboratory, Berkeley, California 94720, USA

Crystalline silicon is an indirect-bandgap semiconductor, making it an inefficient emitter of light. The successful integration of silicon-based electronics with optical components will therefore require optically active (for example, direct-bandgap) materials that can be grown on silicon with high-quality interfaces. For well ordered materials, this effectively translates into the requirement that such materials lattice-match silicon: lattice mismatch generally causes cracks and poor interface properties once the mismatched overlayer exceeds a very thin critical thickness. But no direct-bandgap semiconductor has yet been produced that can lattice-match silicon, and previously suggested structures[1] pose formidable challenges for synthesis. Much recent work has therefore focused on introducing compliant transition layers between the mismatched components[2–4]. Here we propose a more direct solution to integrating silicon electronics with optical components. We have computationally designed two hypothetical direct-bandgap semiconductor alloys, the synthesis of which should be possible through the deposition of specific group-IV precursor molecules[5,6] and which lattice-match silicon to 0.5–1% along lattice planes with low Miller indices. The calculated bandgaps (and hence the frequency of emitted light) lie in the window of minimal absorption in current optical fibres.

Bulk silicon is an indirect-bandgap semiconductor, that is the lowest-energy transition from valence to conduction bands involves a change in crystal momentum. Such materials are typically not suitable for optical applications since nonradiative events dominate the interband transitions. However, silicon is nearly surrounded by direct-bandgap elemental (unary) and compound semiconductors in the periodic table. Moving downwards from Si, the unary group-IV materials acquire larger cores containing *d* electrons; these states affect the conduction band states through orthogonality requirements and changes in the overall volume. On moving from silicon to germanium to tin, the $\Gamma_{2'}$ conduction band (as labelled in silicon) at $k = 0$ drops in energy until, in grey tin, the material acquires a direct (and vanishing) bandgap at $k = 0$. Moving across the periodic table, GaAs, a prototypical direct-bandgap semiconductor, differs from Si or Ge in that the constituents have different electronegativities. The resulting antisymmetric component in the crystal potential flattens the bands and opens the bandgap. In addition, the Γ_6 point of the conduction band drops relative to the other points in the band until it becomes the bottom of the conduction band in most of the well-known direct-bandgap group III–V and II–VI semiconductors.

These well-known results suggest that perhaps one can combine these mechanisms: larger cores and partial ionicity, within alloys containing only group-IV elements wherein the difference in rows of the periodic table provides the contrast in electronegativity. Such a system is likely to require the presence of tin to obtain a direct bandgap[7–10]; the combination of tin (which is substantially larger than silicon) with carbon (which is substantially smaller than silicon) not only affords the greatest contrast in electronegativity

(which is needed to open the zero-bandgap of elemental Sn), but also opens the possibility of tuning the stoichiometry to obtain a lattice match to silicon. Also, the counteracting effects of the larger Sn atoms might compensate for the strain introduced by carbon within a Si/Ge lattice and therefore enhance the solubility of carbon within a silicon and germanium matrix.

To be practical, such an alloy must be accessible to a well-defined synthetic technique. One interesting previous study in computational design[1] has proposed a direct-bandgap lattice-match material. Unfortunately, this material requires the sequential deposition of eight distinct non-interdiffusing monolayers of As/Zn/As/Si/As/Zn/P/Si; this is a formidable synthetic challenge. At first sight, the current proposal for group-IV alloys seems also to present a forbidding synthetic challenge, because tetrahedrally coordinated alloys built from constituents of very different atomic sizes are unlikely to be thermodynamically stable. However, recent synthetic advances[6] allow the production of semiconductor alloys with well-defined (and thermodynamically inaccessible) 1:4 C:Si and C:Ge stoichiometries through the use of precursor molecules which build in the required interatomic bonding, for example, CSi_4H_{12}. The terminal groups (such as H) are eliminated to produce the pure C/Si (or C/Ge) ordered alloy. We can thus produce bulk amounts of metastable alloys of controlled stoichiometry which are not accessible by standard near-equilibrium synthesis methods.

Of particular relevance to the current study are several additional synthetic developments. First, the Sn–D bond has recently been shown to be stable for long periods (at 0 °C) in molecules which incorporate $Sn–D_3$ moieties; (the $Sn–H_3$ moiety, in contrast, is known to be unstable). Second, techniques have been developed to synthesize tetrahedral precursors where a central carbon atom is attached to four tin atoms[11]. Finally, the synthetic yields of CSi_4H_{12} and CGe_4H_{12}, for example, have improved significantly since their discovery, to the range where multi-gram quantities can be regularly prepared[12,13]. Keeping these important advances in mind, we focus on unusual group-IV alloys which can be built from $(Si,Ge,Sn)_4X_{12}$ precursors. In particular, we demonstrate that two alloys, CSi_2Sn_2 and CGe_3Sn, have low-energy allotropes which lattice-match silicon to better than ~0.5–1% and have direct bandgaps. We use the *ab initio* pseudopotential method[14] in the local density approximation (LDA) to calculate both the structural and electronic properties of the proposed group-IV compounds. To obtain the energy gaps more precisely, we also calculate the quasi-particle energy gap using the GW approximation[15].

Figure 1 shows the proposed molecular precursors for CSi_2Sn_2 and CGe_3Sn, namely, $C(SiX_3)_2(SnX_3)_2$ and $C(GeX_3)_3(SnX_3)$ (where X is a terminal group), and the corresponding ordered crystalline phases. These particular crystal structures are the lowest-energy (and highest-symmetry) from among several allotropes with small unit cells built from these precursor molecules. The structures shown are fully relaxed locally and all phonon modes are stable, indicating local structural stability. These $C(AX_3)_{4-x}(BX_3)_x$ molecular precursors maintain the desired tetrahedral bonding. The $CA_{4-x}B_x$ molecular cores also provide the highest possible carbon concentrations without creating energetically unfavourable nearest-neighbour or second-nearest-neighbour C–C pairs[16]. In addition, the absence of strong C–X (such as C–H) bonds allows a low growth

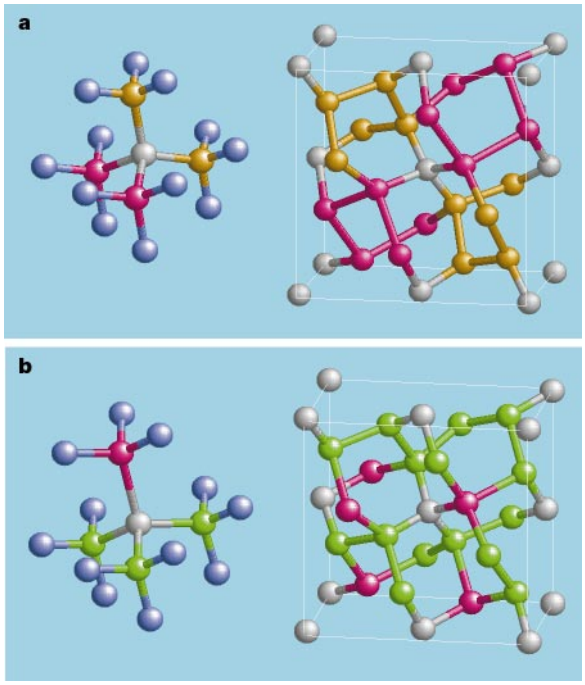

Figure 1 Proposed molecular precursors and the corresponding relaxed crystalline phases of the new group-IV compounds. The crystalline structures shown here are the highest in symmetry among several possible allotropes, and thus are the most plausible structures assumed when depositing on a silicon substrate as discussed in the text. Silicon is yellow, germanium is green, tin is magenta, carbon is grey, and the termination group is light blue. **a**, The molecular precursor $C(SiX_3)_2(SnX_3)_2$ and the corresponding crystal structure CSi_2Sn_2. **b**, The precursor $(GeX_3)_3(SnX_3)$ and the crystal CGe_3Sn. CSi_2Sn_2 has a body-centred tetragonal (b.c.t.) lattice. The three lattice constants are: $a = b = 8.43$ Å, $c = 5.46$ Å. The lattice of CGe_3Sn is slightly distorted from b.c.t., with lattice constants $a = 8.50$ Å, $b = 8.33$ Å, and $c = 5.41$ Å. The angle between a and b is 89.6°

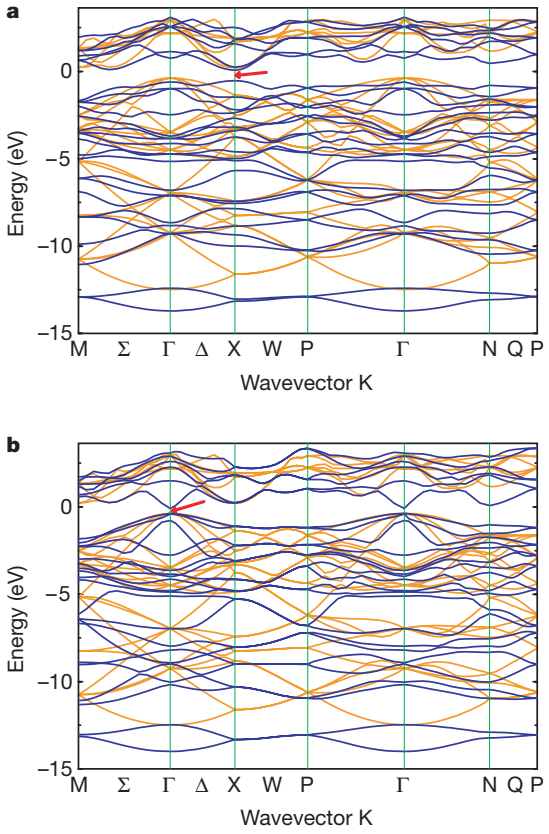

Figure 2 Band structures of novel group-IV alloys compared to that of silicon. The figure shows band structures (in blue) of **a**, CSi_2Sn_2 and **b**, CGe_3Sn. The ionicity opens a bandgap deep in the valence band[19]. Symmetry breaking in CSi_2Sn_2 removes the degeneracy of the X point, pushing one band up significantly so that it becomes the conduction-band maximum and produces in a direct band gap at X (red arrow). In the case of CGe_3Sn, the conduction-band minimum occurs at Γ which produces a direct gap at Γ (red arrow). The band structure of silicon (in orange) calculated in the same unit cell is also plotted for comparison.

temperature which is crucial for synthesizing metastable materials, particularly with tetrahedrally coordinated Sn.

The CSi_2Sn_2 material has a body-centred tetragonal (b.c.t.) lattice with 10 atoms per unit cell. This relatively high-symmetry structure can minimize the anisotropic strains associated with deposition on a low-index silicon surface. The fully relaxed density functional results reveal that the volume per atom in CSi_2Sn_2 is only 0.6% less than that of bulk silicon; (we compare the theoretical LDA volumes to minimize systematic errors). This is only a slight deviation from Vegard's law, which predicts that stoichiometries near $Si_{2.22}Sn_{1.78}C_1$ would lattice-match silicon. The b.c.t. structure of CSi_2Sn_2 provides several lattice planes which can be well-matched to low-index planes of bulk silicon. For example, the (110) and (111) planes of silicon match to CSi_2Sn_2 better than 0.5% in all directions. The 3:1 ratio of noncarbon atomic constituents in CGe_3Sn yields a slightly lower-symmetry structure which is 1.7% lower in volume than bulk silicon. Owing to the lower crystal symmetry, the lattice is slightly distorted from b.c.t. and the best match to silicon is somewhat worse, but still less than 1% in linear dimension (with a combination of compression and dilation along different axes). Mismatches of this order should yield a critical thickness of several hundred or thousand ångstroms (see ref. 17 for example). In addition, a synthesis based on these molecular precursors could allow the addition of a small concentration of a second precursor that helps to tune the lattice match precisely.

Figure 2 compares the pseudopotential density functional band-structures of CSi_2Sn_2 and CGe_3Sn to the corresponding Si band-structure within the same (ten-atom) unit cell. (The specific points X and so on, mentioned below, refer to this ten-atom b.c.t. cell and not the standard two-atom silicon Brillouin zone). CSi_2Sn_2 has a direct bandgap in an unusual position, the X point. The conduction-band minimum at the X point is rather close to the folded X point in Si. Symmetry breaking due to the alloying splits a degeneracy at the X point. In the uppermost valence band, this splitting raises the higher-energy state substantially until it passes the Γ-point state and thereby becomes the new valence-band maximum. This change in the valence-band maximum compared to Si is facilitated by the smaller bandwidths in this more ionic semiconductor alloy. Meanwhile, the conduction band at Γ follows a well-known pattern; the introduction of Sn pulls down the lowest conduction band at Γ and produces a local (but in this case not global) conduction-band minimum at Γ. To understand this somewhat abnormal band structure, that is, a direct energy gap at a point other than Γ, we analyse the charge density at the top valence band for the X and Γ points. At the Γ point, electronic charge is preferentially concentrated around Si–Si bonds. In contrast, at the X point the charge density is higher around the Sn–Sn bonds. Measuring the bond charge contained within fixed-width cylinders, we obtain $(Q_\Gamma(Si\text{–}Si)/Q_\Gamma(Sn\text{–}Sn)) : (Q_X(Si\text{–}Si)/Q_X(Sn\text{–}Sn)) \approx 4 : 1$ (We define the bond charge as the total charge enclosed by a cylinder connecting the two atoms, denoted by the elemental symbol in italics. Although the absolute value of the bond charge scales with the volume of the cylinder, the ratio of the bond charges is insensitive to the cylinder diameter.) Because the valence atomic-orbital energies of Sn are higher than those of Si, the greater Sn character of the X point accounts for the unusual valence-band structure of CSi_2Sn_2. The fundamental LDA bandgap of CSi_2Sn_2 at the X point is 0.59 eV. The GW correction increases the bandgap to 0.9 eV.

The mechanisms which produce a direct bandgap in CGe_3Sn have a more familiar interpretation. Owing to the increased fraction of the lower-row elements Ge and Sn, the drop in the conduction band at Γ is more pronounced than in CSi_2Sn_2. This Γ-point state becomes the new conduction-band minimum, directly above the valence-band maximum, which remains at Γ. The LDA bandgap at Γ is 0.30 eV, increasing to 0.71 eV under the GW correction. The fundamental band gap at Γ is very sensitive to external pressure, dropping by 0.1 volts for a fractional change in volume of $\Delta V/V = 0.01$. This high sensitivity arises from the volume variation in the local potential energy of the conduction band[18] and provides a potentially important mechanism for tuning the size of the direct bandgap.

For consistency, the band structures are calculated at the experimental volume per atom of the posited silicon substrate. Because the volume differences between these materials and bulk silicon are very small, the band structures are very similar to those calculated at their equilibrium volumes. CSi_2Sn_2 shows no significant changes in band structure under such a volume change. The high volume sensitivity of CGe_3Sn means that the small expansion to match the experimental volume per atom of silicon actually drives the bandgap to be direct. (At the relaxed bulk CGe_3Sn volume the bandgap is just slightly indirect.) For CGe_3Sn the optical matrix elements at the direct transition are comparable to those in GaAs. For CSi_2Sn_2, the optical matrix elements are somewhat smaller but the transition is still clearly dipole-allowed.

We have shown how materials design can yield several candidate materials which simultaneously possess three desirable materials properties: a very close lattice match to silicon, a direct bandgap in the 0.7–1.0 V range, and accessibility to well-defined synthetic strategies that can potentially produce bulk quantities of material. □

Received 28 September; accepted 2 November 2000.

1. Wang, T., Moll, N., Cho, K. & Joannopoulos, J. D. Deliberately designed materials for optoelectronics applications. *Phys. Rev. Lett.* **82,** 3304–3306 (1999).
2. Ejeckam, F. E., Lo, Y. H., Subramanian, S., Hou, H. Q. & Hammons, B. E. Lattice engineered compliant substrate for defect-free heteroepitaxial growth. *Appl. Phys. Lett.* **70,** 1685–1687 (1997).
3. Lo, Y. H. New approach to grow pseudomorphic structures over the critical thickness. *Appl. Phys. Lett.* **59,** 2311–2313 (1991).
4. Powell, A. R., Iyer, S. S. & LeGoues, F. K. New approach to the growth of low dislocation relaxed SiGe material. *Appl. Phys. Lett.* **64,** 1856–1858 (1994).
5. Kouvetakis, J., Nesting, D. & Smith, D. J. Synthesis and atomic and electronic structure of new Si-Ge-C alloys and compounds. *Chem. Mater.* **10,** 2935–1949 (1998).
6. Kouvetakis, J., Chandrasekhar, D. & Smith, D. J. Growth and characterization of thin $Si_{80}C_{20}$ films based upon Si_4C building blocks. *Appl. Phys. Lett.* **72,** 930–932 (1998).
7. Jenkins, D. W. & Dow, J. D. Electronic properties of metastable Ge_xSn_{1-x} alloys. *Phys. Rev. B* **36,** 7994–8000 (1987).
8. Mäder, K. A., Baldereschi, A. & von Känel, H. Band structure and instability of $Ge_{1-x}Sn_x$ alloys. *Solid State Commun.* **69,** 1123–1126 (1989).
9. He, G. & Atwater, H. A. Interband transitions in Sn_xGe_{1-x} alloys. *Phys. Rev. lett.* **79,** 1937–1940 (1997).
10. Min, K. S. & Atwater, H. A. Ultrathin pseudomorphic Sn/Si and Sn_xSi_{1-x}/Si heterostructures. *Appl. Phys. Lett.* **72,** 1884–1886 (1998).
11. Klinkhammer, K. W., Kühner, S., Regelmann, B. & Weidlein, J. Die Kristall- und Molekulstruktur von Tetrakis(trimethylstannyl)methan. *Organomet. Chem.* **496,** 241–243 (1995).
12. Schmidbaur, H. & Zech, J. An improved synthetic pathway to tetrasilyl methane and the synthesis of disilylpropane. *Eur. J. Solid State Inorg. Chem.* **29,** 5–21 (1992).
13. Kouvetakis, J. *et al.* Novel methods for CVD of Ge_4C and $(Ge_4C)_xSi_y$ diamond-like semiconductor heterostructures: Synthetic pathways and structures of trigermyl-$(GeH_3)_3CH$ and tetragermyl-$(GeH_3)_4C$ methanes. *J. Am. Chem. Soc.* **120,** 6738–6744 (1998).
14. Ihm, J., Zunger, A. & Cohen, M. L. Momentum-space formalism for the total energy of solids. *J. Phys. C* **12,** 4409–4423 (1979).
15. Hybertsen, M. S. & Louie, S. G. Electron correlation in semiconductors and insulators: Band gaps and quasiparticle energies. *Phys. Rev. B* **34,** 5390–5413 (1986).
16. Rücher, H., Metthfessel, M., Bugiel, E. & Osten, H. J. Strain-stabilized highly concentrated pseudomorphic $Si_{1-x}C_x$ layers in Si. *Phys. Rev. Lett.* **72,** 3578–3581 (1994).
17. Herman, M. A. & Sitter, H. *Molecular Beam Epitaxy: Fundamentals and Current Status* (Springer, Berlin/Heidelberg, 1989).
18. Corkill, J. L. & Cohen, M. L. Band gaps in some group-IV materials: A theoretical analysis. *Phys. Rev. B* **47,** 10304–10309 (1993).
19. Cohen, M. L. & Chelikowsky, J. R. *Electronic Structure and Optical Properties of Semiconductors* (Springer, Berlin/Heidelberg, 1988).

Acknowledgements

V.H.C. thanks T. Mallouk and J. Kouvetakis for useful discussions and J. Kouvetakis for information on the stability of Sn-D_3 moiety. V.H.C. acknowledges support from the Packard Foundation and from the National Science Foundation, Division of Materials Research. V.H.C. also acknowledges the National Partnership for Advanced Computational Infrastructure and the Pittsburgh Supercomputing Center for computational support. M.L.C. and S.G.L. acknowledge support from the National Science Foundation, Division of Materials Research and from the Office of Energy Research, Office of Basic Energy Sciences, Materials Sciences Division of the US Department of Energy.

Correspondence and requests for materials should be addressed to V.H.C. (e-mail: crespi@phys.psu.edu).